C3A Cell Behaviors on Micropatterned Chitosan-Collagen-Gelatin Membranes

Bo-Yi Yu, Pei-Hsun Chou, Chang-An Chen, Yi-Ming Sun, Shieh-Shiuh Kung

C3A Cell Behaviors on Micropatterned Chitosan–Collagen–Gelatin Membranes

BO-YI YU,[1] PEI-HSUN CHOU,[1] CHANG-AN CHEN,[1]
YI-MING SUN[1,2,*] AND SHIEH-SHIUH KUNG[2]
[1]*Department of Chemical Engineering and Materials Science*
[2]*Graduate School of Biotechnology and Bioinformatics*
Yuan Ze University, Chungli, Taoyuan, Taiwan 320, Republic of China

ABSTRACT: The influence of the properties and surface micropatterning of chitosan–collagen–gelatin (CCG) blended membranes on C3A cell's activities has been investigated. It is aimed to guide the cell growth and improve the growth rate *in vitro* for the application in tissue engineering. Masters with micropatterns are prepared on stainless steel plates by photolithography. The CCG membranes with surface micropatterns are then fabricated by soft lithography and dry–wet phase inversion techniques. The morphology and metabolic activity of cultured C3A cells on the membranes are recorded. When the C3A cells are seeded on the membranes with micropattern spacing of 200 μm width and 80 μm depth, they adhere and aggregate in the groove of the membranes in a few minutes. The aggregated cells migrate up to the surface of the ridge later. This phenomenon, however, is not found on membranes with a micropattern spacing of 500 μm width. In addition, it is demonstrated that the cells on the CCG membranes with micropatterns have higher metabolism and growth rates than those on the flat CCG membranes and on T-flask discs. Micropatterning on the membrane surface can affect the distribution of cells and the communication among cells, and results in a difference in cell adhesion, morphology, mobility, and growth activity.

KEY WORDS: biomaterials, cell–material interactions, chitosan–collagen–gelatin and micropatterning.

*Author to whom correspondence should be addressed.
E-mail: cesunym@saturn.yzu.edu.tw
Figures 1–3 and 5 appear in color online: http://jba.sagepub.com

0885-3282/07/03 0255–20 $10.00/0 DOI: 10.1177/0885328207076780

Los Angeles, London, New Delhi and Singapore

INTRODUCTION

In recent years, microfabrication techniques have received great attention in biotechnology, such as biochips, biosensors, scaffolds in tissue engineering, drug delivery systems, and fundamental studies of cell biology [1]. Positioning of cells on substrate is also important for cell-based diagnostic screening.

Tissue engineering is the regeneration, replacement, or restoration of human tissue function by combining synthetic/natural materials and biomolecules in appropriate configurations and environments [2,3]. The scaffold, cells, and necessary growth factors are three major components in any tissue-engineered construct. Tissue engineering may require that cells be placed in specific locations to create organized structures. For example, functional nerves or blood vessels form only when groups of cells are organized and aligned in very specific geometries.

Patterning techniques that control both the size and shape of regions on a substrate surface with difference in chemistry or topology, are extremely useful in understanding the influence of the cell–materials interface on the behavior of cells [1,4]. The technique can also benefit cell co-culture that helps one better understand the interaction of cells with other cells [5].

In addition, biocompatibility has been associated with surface microtopography, microtexture, and microchemistry. Surface chemistry and topography ultimately affect the nature and the strength of cell–cell and cell–material interactions occurring at the culturing environment [6] (e.g., water and ion sorption, protein adsorption, cell adhesion, mobility, spreading, and proliferation). Adhesion, proliferation, and function of anchorage dependent cells are highly related to the surface properties of the biomaterials. It is widely accepted that the physico-chemical properties of the material surface determine the adsorption of proteins and subsequent cell interactions [7–9].

Polymeric materials possess a number of attractive properties, such as processibility, durability, and optical clarity that make them suitable for BioMEMS devices [10]. Specifically, some of them also possess excellent biocompatibility and can provide various biofunctionalities. Proper combinations of polymers and biomolecules may offer tailored properties for a variety of biomedical applications. Chitosan, collagen, and gelatin are biological polymers obtained from nature. They are biodegradable, biocompatible, and immunogenic and have been widely accepted for biomedical applications. They can be blended together to form

a structure that mimics extracellular matrix (ECM) *in vitro* [11,12]. Gelatin includes the peptides of Arg-Gly-Asp (RGD) sequence that can enhance cells adhesion; it also can form a polyelectrolyte complex (PEC) with chitosan at suitable pH levels when used as a scaffold for tissue engineering [11–15].

Soft lithography was invented by Whiteside and his coworkers who fabricated stamps or channels on a surface of an elastomeric ('soft') material for pattern transfer or modifications [16–18]. The elastomeric material is poly(dimethylsiloxane) (PDMS) and it has several properties that make it suitable for surface patterning on biomaterials. PDMS is a biocompatible, non-toxic, durable, and inexpensive silicon-based inorganic polymer, and its low surface energy does not allow it to adhere to other materials. Hence it can be easily separated from delicate master molds with fine patterns. It can be used to transfer patterns onto three-dimensional structures. As numerous replicas can be generated from a single master and each replica can be used more than once, one can get a large amount of products with the advantages of low cost, time-saving, and reproducibility in rather simple operations [17,18].

C3A cells have been accepted as model cells for the study of liver regeneration *in vitro*. C3A cell is a patented human liver cell line derived from the hepatoblastoma tumor of early childhood. The cells perform about the same functional activity as human primary hepatocytes on a per-gram basis. The advantages of using this cell line instead of using rat or porcine hepatocyte primary cells include cell stability, ease of proliferation, and long-term maintenance [19–21]. Moreover, C3A cells were shown to be applicable in a biohybrid liver support system [22,23].

In order to discuss the relationship of two kinds of cells, Kang et al. [24] and Fukuda et al. [25] fabricated chemical micropattern on glass wafer by using light lithography. But the glass wafer had a limitation that it could not be used *in vivo*, and the impact of surface topological micropatterning on cells was not discussed. In this article, the influence of the surface topological micropatterning on the chitosan–collagen–gelatin (CCG) blended membranes on the C3A cell's activities is reported. Its aim was to guide the growth and improve the growth rate of C3A cells in the culturing environment for the application in tissue engineering. The CCG membranes with surface micropatterns were prepared by soft lithography and dry–wet phase inversion techniques. The micropatterned CCG membranes were characterized, the culturing of C3A cells on the membranes was recorded, and the bioactivities of the cells on the membranes were analyzed.

EXPERIMENTAL DETAILS

Preparation of Micropatterned Membranes

Master

Micropatterns were fabricated on the surface of a stainless steel (S.S.) plate via photolithography. The mask was designed by using AutoCad. The surface of the S.S. plate was coated with a positive photoresist, and then exposed to UV light through the mask. The portion of photoresist exposed to UV light and the underlying S.S. surface could be washed or etched away with a ferrous chloride solution. The S.S. master contained parallel ridges and grooves with spacing of 200 or 500 μm and 80 μm in depth on its surface.

Elastomer Stamp

The silicone rubber stamp was made from Dow Corning 1540/20P. The PDMS prepolymer and curing agent were mixed at a ratio of 10 : 1 and then cast on the S.S. master plate. The cast solution and the plate were placed in vacuum to remove trapped bubbles. The silicone rubber stamp was cured at 70°C for 3 h. It can be easily removed from the master afterwards.

Surface-micropatterned Membranes

The surface-micropatterned CCG membranes were prepared by replication of the micropatterns on the silicone rubber stamp. The membrane casting solution was prepared by mixing 3 g chitosan (Sigma, C-3646, minimum 85% deacetylated), 3 g collagen (Dgf Stoess, Gelita-Sol D aggl.), and 3 g gelatin (provided with courtesy from Dah Feng Capsule Industry, Inc., Taichung, Taiwan) in a flask that contained 100 mL 2% aqueous acetic acid solution. The mixture solution was stirred at 180 rpm at 50°C for 24 h, and then kept stationary for 24 h in order to eliminate air bubbles. The polymer solution was poured onto the silicone rubber stamps, which was placed in plastic petri dishes, kept at 70°C for 3 h, and then treated with NaOH solution (2%) to neutralize the acetic acid. During this time the membranes spontaneously released from the stamps. The micropatterns on the stamp surface were replicated to the membranes. A schematic of the micropatterned membrane preparation procedures is shown in Figure 1. The membranes were repeatedly washed with deionized water, immersed into 70% ethanol aqueous solution overnight, and then exposed to UV light for sterilization. The sorbed ethanol was then removed by soaking and washing with phosphate-buffered solution (PBS).

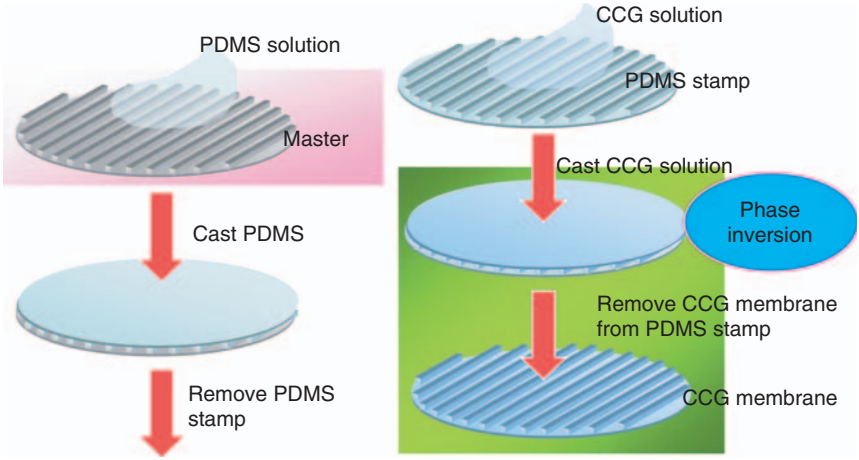

Figure 1. The schematic outline of the soft lithography and dry–wet phase inversion methods in the fabrication of micropatterns on CCG membranes.

Atomic Force Microscopy (AFM)

The surface topography of the membrane with micropatterns was characterized by atomic force microscopy (AFM, Shimadzu, SJ9500) using intermittent mode. Root mean square (RMS) roughness of a representative $15 \times 15\,\mu m^2$ section was calculated using Shimadzu software, and the formula is:

$$R_a = \frac{1}{L_x L_y} \int_o^{Ly} \int_0^{Lx} |f(x,y)| = d_x d_y.$$

C3A Cell Culture and Seeding

The C3A cells (from a human hepatoblastoma cell line) were supplied by the Food Industry Research and Development Institute (FIDRI, Taiwan). The culture medium was Eagle MEM (Sigma) supplement solution with 10% fetal bovine serum (HyClone-SH30071.03), 1% sodium pyruvate (Sigma), 0.1% amphotericinc (Sigma), and 1% Penicillin-G (Sigma). Surface-micropatterned membranes were placed in 24-well tissue culture palates (Orange). The membranes were cut into 13 mm-diameter discs and were tightly wedged into the culture wells. To prevent the membrane from floating in the presence of the medium,

Teflon O-rings were used to fix the membranes to the bottoms of the wells. After the culture medium was placed in the wells, the cells were seeded at a density of 2×10^4 cells per well. The cell containing solution (0.1 mL) was dropped onto the center of each membrane. With gentle shaking, the cells would spread over the surface of the CCG membrane. The cells were cultured in a humidified incubator in the presence of 5% CO_2 at 37°C.

In order to discuss the binding interaction of cells with the substrate, the cell loading time and the trypsin detachment time were determined for the cells cultured on the flat CCG membranes and TCPS. Cell loading time is the time required for cell adhesion or immobilization on the membrane surface. It was determined when the cells were no longer floating around the medium and fixed on the substrate surface after seeding. It is well known that cells can be harvested from a culturing substrate by adding trypsin to cleave the peptide bonding between the cells and the substrate surface. The trypsin detachment time is the time required for the cells to detach from the membrane surface after trypsin was added to the culture medium. Both times were determined through the observation of the culture by using a phase contrast microscope.

Morphology of the C3A cells

An inverted optical microscope equipped with a CCD camera was operated in phase contrast mode to follow the morphology of the cells in real time. The CCG membranes are transparent so that clear images of cells can be observed. A scanning electron microscope (SEM) was used to observe finer images of the cultured cells. The cells on the membranes were fixed with 2.5% glutaraldehyde and 1% OsO_4 (Sigma); all the procedures were done at 4°C. The samples were then dehydrated in graded ethanol of 50, 70, 80, 90, and 95 vol%, twice with absolute ethanol, finally they were dried using a CO_2 critical-point-drier (CPD). The samples were sputtered with gold and observed with a scanning electron microscope (JSM-5600, Jeol) at an acceleration voltage of 20 kV.

Cell Activities

The activities of the C3A cells were determined using 3-(4,5-dimethylthyl-2-thiazolyl)-2,5-diphenyl-tetrazolium bromide (MTT), ammonia, albumin assays after 3 days of culturing. A MTT assay, which assesses the rate of mitochondrial reduction of MTT, was used to measure the relative proliferation activity of cells. The MTT assay kit was obtained from KPL and used following the procedures suggested by

the supplier. Each test was quadruplicated by using an ELISA reader (Thermo Lab systems) [26,27]. Ammonia and albumin were two metabolites produced during cell growth. The ammonium concentration was detected by a UV-Vis spectrophotometer at a wavelength of 630 nm. Before the albumin secretion measurement, the wells with cultured cells were washed with serum-free medium and finally filled with 500 μL FBS-free medium. The medium was withdrawn from the wells after replacing the medium for a day and the amount of secreted albumin protein was determined. Albumin production was determined by ELISA reader.

Statistic Analysis

Statistical evaluations of the data were performed using one-way ANOVA with SPSS. Statistics < 0.05 were considered statistically significant.

RESULTS

The parallel ridge and groove patterns on the stainless steel master were produced by photolithography and the pictures of the micropatterns are shown in Figure 2(a). The surface of the patterns was smooth and matched the original design. However, the depth was limited to 80 μm because of the etching strength of ferrous chloride solution used. The micropatterns on the silicone rubber got good replication from the master as shown in Figure 2(b). When the CCG blended polymer solution was cast on the stamp, it followed a phase inversion process and formed a transparent membrane with micropatterns on its surface. Figure 2(c) shows the pictures of a CCG membrane with micropatterns transferred from the patterns of silicone rubber surface. The results demonstrated that micropatterned CCG membranes in 200 μm could be fabricated reproductively by using soft lithography. A large number of test samples could be prepared easily with this technique. The blended materials were biocompatible, biodegradable, and suitable for cell adhesion and proliferation. Adjusting the polymer composition/concentration and processing conditions could further optimize the properties of micropatterned membranes. Currently, surface micropatterns with 10–20 μm in spacing can be well prepared with the modified processing conditions in the laboratory (not shown).

The surface roughness of the membrane surface with micropatterns was measured by atomic force microscopy (AFM). The results showed

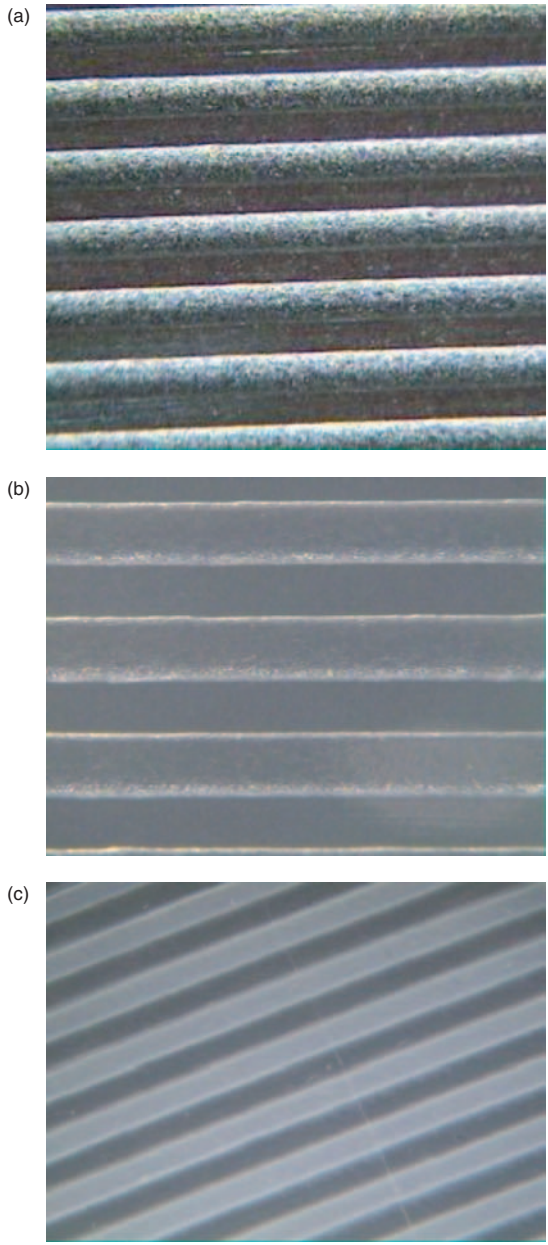

Figure 2. The micropatterns on the substrate of: (a) the stainless steel master; (b) the PDMS stamp and (c) the CCG membrane. The feature of the micropatterns are parallel ridge and groove with a spacing of 200 μm and a depth of 80 μm.

that the surface roughness on different positions varied remarkably. Figure 3(a) shows the surface topography on the groove of micropatterns and the mean surface roughness was about 260 nm. Figure 3(b) shows the surface topography on the ridges and the mean surface roughness was 157 nm. The surface in the groove was rougher than that on

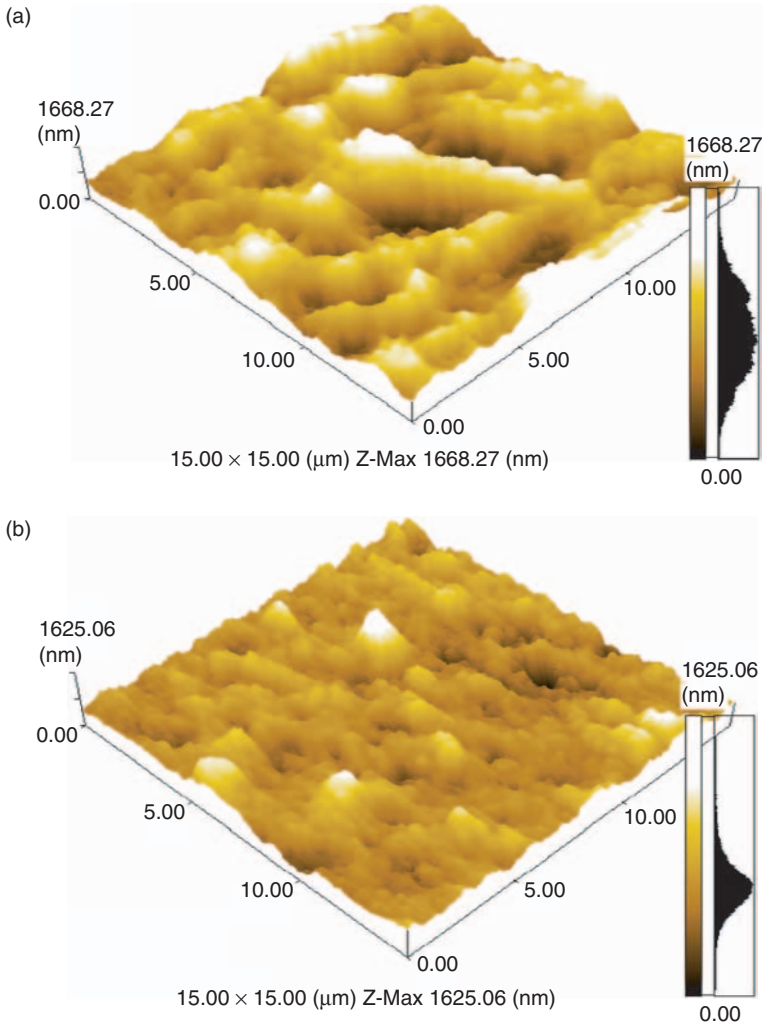

Figure 3. The topography of the micropatterned CCG membrane surface determined by AFM: (a) groove and (b) ridge.

the ridge. The results were reasonable since the groove surface was a replica of the etched surface on the S.S. master. An etched surface was rougher than the original surface of the S.S. plate. The roughness was transferred to the ridge of the micropatterns on silicone rubber and then to the groove of the micropatterns on CCG membranes.

The CCG blended membrane is a good ECM substrate for cells to adhere, spread, and proliferate *in vitro*. Figure 4(a) and (b) shows the SEM pictures of C3A cells (seeding density: 2×10^4 cells/well) after culturing on the CCG membrane for 5 days. Most of the cells adhered,

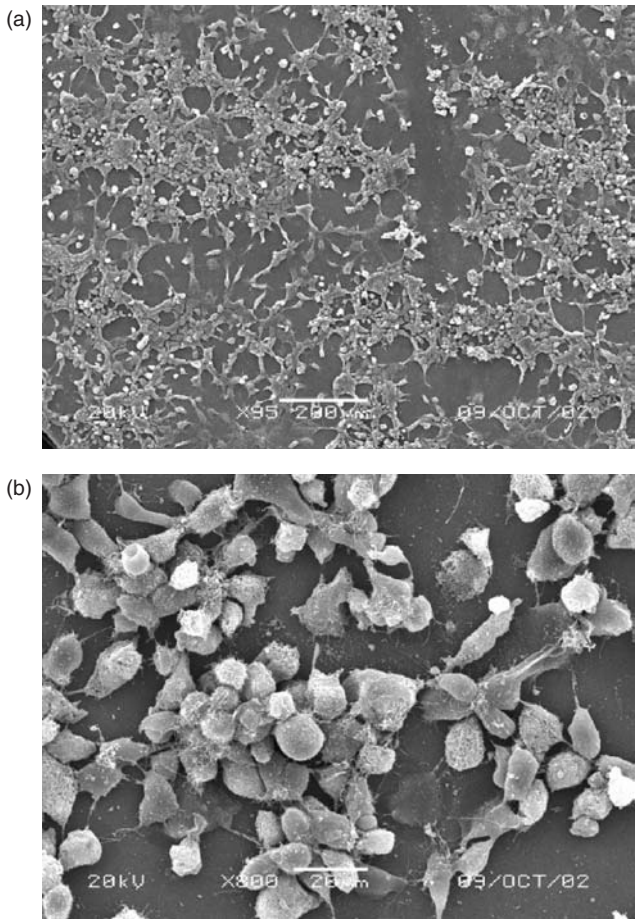

Figure 4. Scanning electron micrographs of C3A cells cultured on the CCG membrane after 5 days (×95).

spread, and changed their shapes from spherical to spindly. Many of them touched and connected with each other via the tail end of their spindly bodies. In the meantime, some of the cells were still round, and there was a nonuniform distribution of clumps of cells (Figure 4(b)). However, these pictures demonstrated that all the cells developed different morphology after seeding and CCG membranes could be used as a substrate for culturing of C3A cells in a later study.

In addition, the binding interaction or adhesion of C3A cells with the CCG membranes was stronger than that with TCPS. The time for C3A cells to adhere on a CCG membrane was much shorter than that on a TCPS surface, and the time required for trypsin to separate the cells from a CCG membrane was much longer than that from a TCPS surface (Table 1). The positively charged surface of the CCG membrane accounted for these results, as it may have attracted the negative charges on the surface of cells. The effect not only shortened the time for cells to deposit on the surface of the CCG membrane but also provided a strong binding force between cells and the membrane surface.

The size of the micropatterns could affect the distribution and behaviors of C3A cells. As the CCG membranes were transparent, one could directly observe the morphology of the cells using a phase-contrast optical microscope. Figure 5(a) shows the C3A cells cultured on the micropatterned membranes of 200 μm scale at a seeding density of 2×10^4 cells/well. The distribution of the cells on the patterned membrane surface was not uniform since seeding. Most of the cells aggregated in the groove, and only a small amount of them settled on the ridges. However, the cell distribution was much more even on the membrane surface of larger scale micropatterns. Figure 5(b) shows the C3A cells cultured on the micropatterned membranes of 500 μm scale at a seeding density of 2×10^4 cells/well. The distribution of the cells was quite uniform in the groove or on the ridge; in other words, the

Table 1. Time required for C3A cells to deposit on and be removed by trypsin from the CCG membrane or TCPS surfaces. Cell loading time meant when seeding cells on the substrate, how much time the cells could not move with fluid flow. Trypsin detachment time meant when using trypsin to harvest cells, how much time the cells could all separate from substrate. The situations of cells on the substrate could be obtained by using phase contrast microscopy in both the experiments.

	CCG membrane	TCPS
Cell loading time (min)	<5	>180
Trypsin detachment time (min)	>90	>10

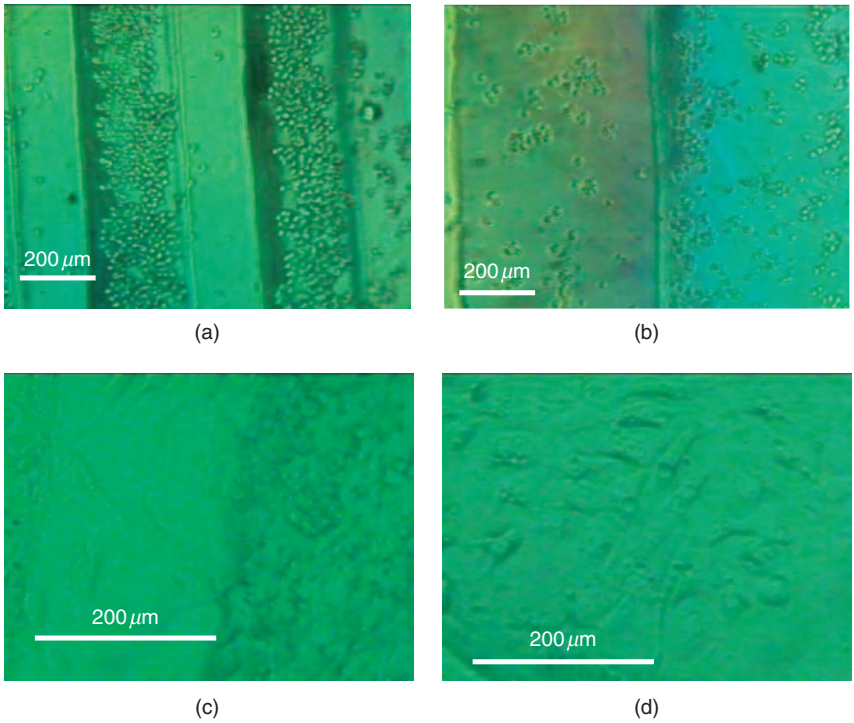

Figure 5. The optical micrographs of the C3A cells cultured on the CCG membranes with micropatterns of: (a) 200 μm scale (after seeding for 15 min); (b) 500 μm scale (after seeding for 15 min); (c) 200 μm scale (after seeding for 24 h) and (d) 500 μm scale (focused in the groove after seeding for 24 h).

micropattern in a scale of 500 μm did not affect the distribution of the cells. After culturing for 24 h, the cells proliferated and differentiated in their morphology (from spherical to spindly), as shown in Figure 5(c) and (d). On the micropatterned surface of 200 μm scale, they occupied the entire surface in the groove, and migrated up to the ridge (Figure 5(c)). The cells in the groove of the 500 μm scale spread and occupied a great portion of the groove surface (Figure 5(d)), and the cells on the ridge behaved similarly (not shown).

Two kinds of cell morphologies were developed on the different portions (groove or ridge) of the micropatterned surface. The scanning electric micrographs gave better morphology information of the cells. Figure 6(a)–(c) shows the C3A cells cultured on the micropatterned membranes with a scale of 200 μm at a seeding density

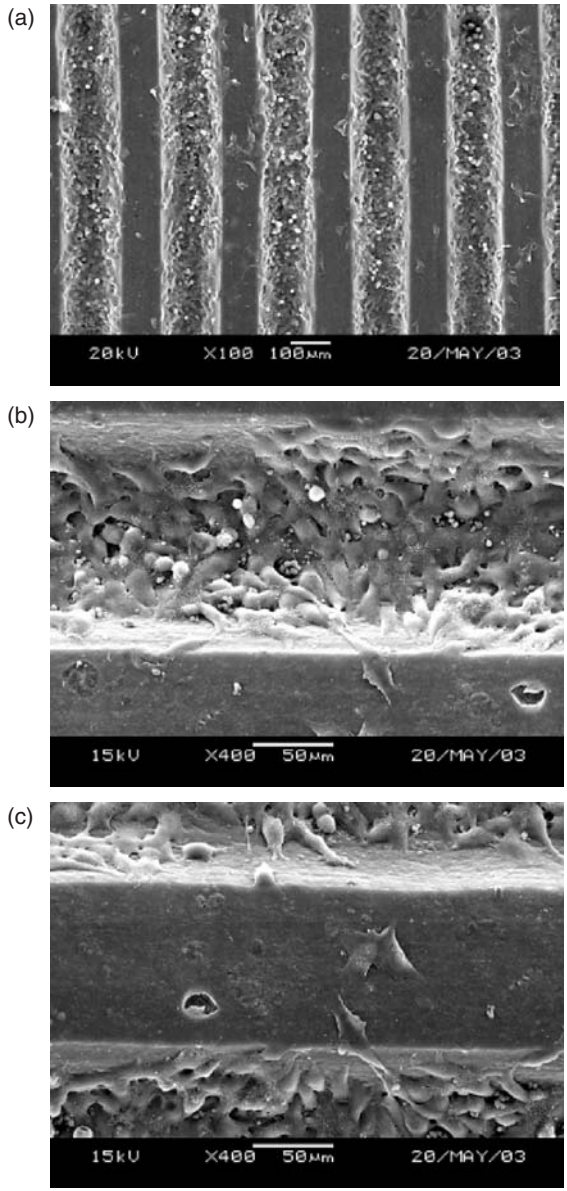

Figure 6. Scanning electron micrographs of the C3A cells cultured on the CCG membranes with micropatterns of 200 µm scale: (a) an overview after seeding for 24 h; (b) focused in the groove after seeding for 24 h; (c) focused on the ridge after seeding for 24 h; (d) an overview after seeding for 48 h; (e) focused on the ridge after seeding for 48 h and (f) focused on the ridge after seeding for 72 h.

(d)

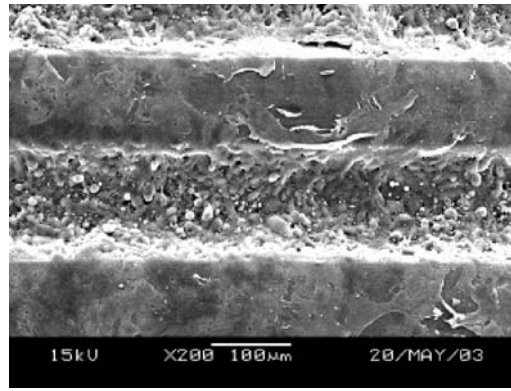

(e)

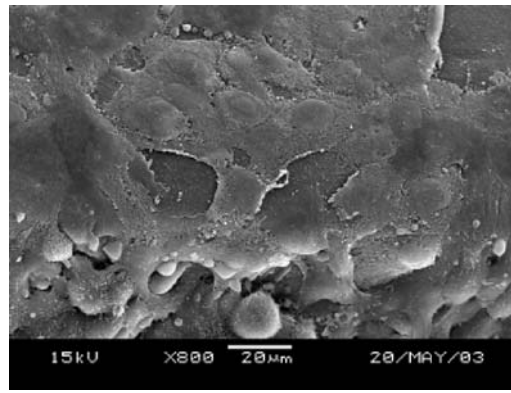

(f)

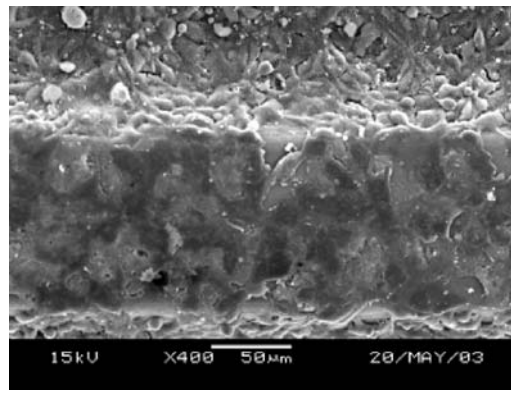

Figure 6. Continued.

of 2×10^4 cells/well, after 24 h. The cells in the groove were spindly and covered most of the bottom surface and began to migrate up to the ridge. In contrast, the cells on the ridge were flat and they were sparsely distributed on the surface. After seeding for 48 h, the cells in the groove still looked similar to those at 24 h, but a greater number of cells had gathered on the ridge, as shown in Figure 6(d) and (e). It seemed that a number of cells had migrated to the surface of the ridge from the groove. After seeding for 72 h, the cells on the surface of the ridge piled up; in other words, the thickness of the cell layers increased with time, as shown in Figure 6(f). It should be noted that the cells behaved remarkably different from those cultured on the flat CCG membranes as shown in Figure 4(a) and (b). Cells were highly densified in the grooved region on the patterned surface although the initial seeding density was the same.

The activities of C3A cells were determined using MTT, ammonia, and albumin assays after 3 days of culturing. The ammonia and albumin assays represent the overall metabolic activity or growth rate of C3A cells. The higher ammonia or albumin concentration indicated that the cells might have higher cell growth rate or overall metabolic activity. The cells on the patterned membrane created a higher ammonia concentration (21.0 μL/L) than both those on the flat membrane (17.7 μL/L) and the reference (14.5 μL/L) as shown in Figure 7(a). Similar results were found for albumin assay. The cells on the patterned membrane resulted in a higher albumin concentration (1.02 μL/L) than those on the flat membrane (0.62 μL/L) and the reference (0.48 μL/L) as shown in Figure 7(b). MTT assay is used to determine disruption of a critical biochemical function, and it also indicates the proliferation activity of the cells. This assay quantifies mitochondrial activity by measuring the formation of a dark blue formazan product formed by the reduction of the tetrazolium ring of MTT [26,27]. The cells on the CCG membranes (patterned or flat) showed higher MTT values than those on the TCPS reference, but the cells on the flat or patterned membranes did not show significant difference, as shown in Figure 7(c). The result was consistent with the results of ammonia and albumin assays.

DISCUSSION

In this study, it has been found that the membrane with micropatterns in 200 μm scale could influence the distribution of C3A cells in seeding. Most of them aggregated in the groove, and few settled on the ridge. It was suspected that this was related to the cell moving distance after the cells touched the membrane surface. The cells were spherical and could

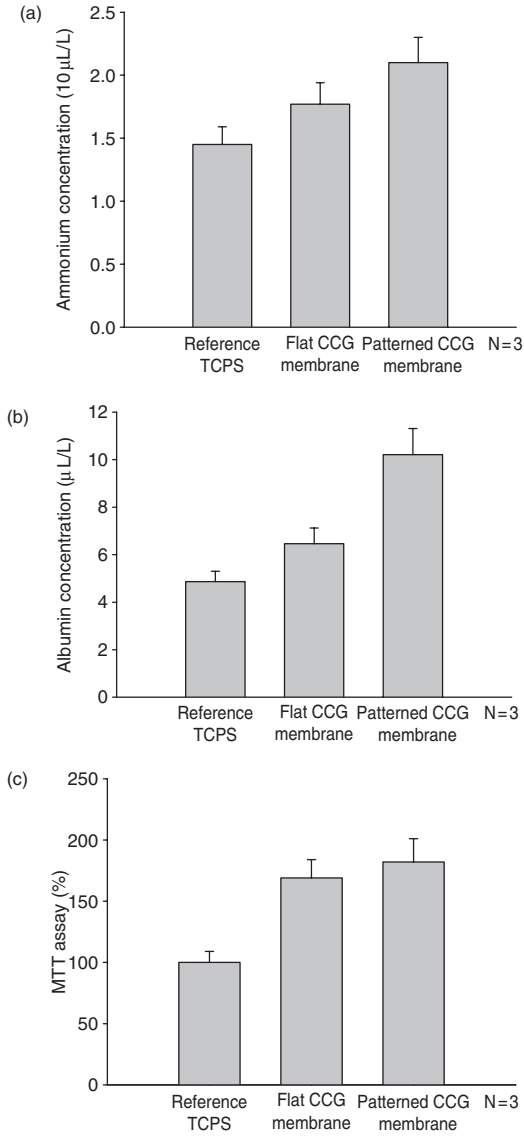

Figure 7. The metabolic and growth activities of C3A cells on different substrates in terms of (a) ammonium secretion; (b) albumin secretion and (c) MTT assay. The seeding density was 2×10^4 cells per well and the data were taken at 72 h after seeding. The ANOVA test was applied by using SPSS software, and the F values of (a) ammonium assay; (b) abumin assay and (c) MTT assay were 15.68, 64.13, and 33.27. All of them were greater than the value of $F_{2,\ 6,\ 0.05}$, 5.14, (**P values <0.05). It proved the data obtained were meaningful.

bounce or roll like balls on the surface in the beginning of cell seeding. However, the membrane surface was not frictionless because it was covered with cell adhesion proteins, which were deposited from the medium. The bouncing or rolling cells may have stopped moving due to the protein adhesion effect. If the average moving distance was shorter than the width of the ridge, most of the cells would fall into the groove. The cells would be trapped there, as the groove was 80 μm in depth. In addition, the surface in the groove was rougher than that on the ridge so that cells may have been able to anchor in the groove easier. It was speculated that the average moving distance of the cells was >200 μm but was <500 μm on the surface of the ridge. The non-uniform distribution of the cells on the micropatterns of 500 μm scale was not observed.

The C3A cells wound develop specific morphology according to the topological environment they encountered. The amount of the gathered cells would affect the communication and signal transmittance among cells. The cells on the ridge were scattered sparsely; they differentiated to a leafy morphology and tended to develop pseudopodia in order to outreach other cells and improve communication among them. The cells in the groove were close to each other; they communicated with each other easily and could proliferate to a much larger number of regular spindly cells. In a longer time later after seeding, some of the cells in the groove began to migrate up to the ridge and changed their morphology to flattened slices. The result demonstrated that the C3A cells could develop to different morphologies via a self-regulating process according to the topological difference on the same surface of materials. Similar results were obtained for PC12 cells under the same culturing conditions (data not shown).

In the later stage of culturing, the cells began to move up to the ridge and the morphology of them became abnormal flat strips (Figure 6(c)–(f)). One might wonder that if they were in a process of apoptosis. Ren et al. [28] indicated that apoptotic cells would round up and fragment into multiple residues and the chromosome showed condensation and aggregation around the periphery of the nucleus. There was very little interaction between apoptotic cells and the material surface. The preservation of cellular membrane and organelles was one of the most reliable markers of apoptosis. The cells in this culture were still lacking those behaviors. In addition, the cells on the ridge could respond to the presence of as morphology of the cells became globular (picture not shown). In fact, it was suspected that cells might function differently or change to specific morphology when they encounter a different environment. The details of those phenomena and their rationalization will be worth future study.

CONCLUSIONS

The surface micropatterns in 200 μm scale would affect the distribution of the C3A cells and the cells could develop different morphologies according to the topological environment on the same materials. In addition, C3A cells on the micropatterned surface of CCG membranes had better growth and metabolic rates than those on the flat CCG membranes or TCPS. However, it is still not clear that how the micropatterns influence the signal transmittance among cells and regulate the growth or metabolic activities of the cells. It will be of interest to further discuss the cell–cell and cell–material interactions from the cell biological point of view in the future. The knowledge of the effects of smaller size scales of the micropatterns or even nanopatterns on the cell adhesion, spreading, migration, differentiation, and proliferation will be of importance in the regulation and manipulation of cell culture *in vitro* for the application in tissue engineering. The surface micropatterns also have the potential for co-culturing of multiple cells and cell bioreactor design. There remained many fundamental and practical problems for further study.

ACKNOWLEDGMENT

This work was supported by the National Science Council of the Republic of China through the grant of NSC92-2216-E-155-001. The authors would like to thank Professor Jyh-Ping Chen of Chang Gung University for his kind help on initializing the cell culture experiments.

REFERENCES

1. Lee, L.J. (2003). BioMEMs and Micro-/Nano-processing of Polymers – An Overview, *J. Chin. Inst. Chem. Engrs.*, **34**(1): 25–46.
2. Nikolovski, J. and Mooney, D.J. (2000). Smooth Muscle Cell Adhesion to Tissue Engineering Scaffolds, *Biomaterials*, **21**(20): 2025–2032.
3. Griffith, L.G. and Noughton, G. (2002). Tissue Engineering-Current Challenges and Expanding Opportunities, *Science*, **295**(5557): 1009–1014.
4. Manwaring, M.E., Walsh, J.F. and Tresco, P.A. (2004). Contact Guidance Induced Organization of Extracellular Matrix, *Biomaterials*, **25**(17): 3631–3638.
5. Yamato, M., Konno, C., Utsumi, M., Kikuchi, A. and Okano, T. (2002). Thermally Responsive Polymer-Grafted Surfaces Facilitate Patterned Cell Seeding and Co-Culture, *Biomaterial*, **23**(2): 561–567.

6. Massia, S.P. and Hubbell, J.A. (1992). Immobilized Amines and Basic Amino Acids as Mimetic Heparin-Binding Domains for Cell Surface Proteoglycan-Mediated Adhesion, *J. Biological Chem.*, **267**(14): 10133–10141.
7. Grinnell, F., Milam, M. and Spree, P.A. (1973). Attachment of Normal and Transformed Hamster Kidney Cells to Substrata Varying in Chemical Composition, *Biochem. Med.*, **7**(1): 87–90.
8. Anselme, K. (2000). Osteoblast Adhesion on Biomaterials, *Biomaterials*, **21**(7): 667–681.
9. Krasteva, N., Harms, U., Albrecht, W., Seifert, B., Hopp, M., Altankov, G. and Groth, T. (2002). Membranes for Biohybrid Liver Support Systems-Investigations on Hepatocyte Attachment, Morphology and Growth, *Biomaterials*, **23**(12): 2467–2478.
10. Griffith, L.G. (2000). Polymeric Biomaterials, *Acta Mater.*, **48**(1): 263–277.
11. Mao, J.S., Zhao, L.G., Yin, Y.J. and Yao, K.D. (2003). Structure and Properties of Bilayer Chitosan-Gelatin Scaffolds, *Biomaterial*, **24**(6): 1067–1074.
12. Zhao, F., Yin, Y., Lu, W.W., Leong, J.C., Zhang, W., Zhang, J., Zhang, M. and Yao, K. (2002). Preparation and Histological Evaluation of Biomimetic Three-Dimensional Hydroxyapatite/Chitosan-Gelatin Network Composite Scaffolds, *Biomaterials*, **23**(15): 3227–3234.
13. Yin, Y.J., Yao, K.D., Cheng, G.X. and Ma, J.B. (1999). Properties of Polyelectrolyte Complex Films of Chitosan and Gelatin, *Polym. Int.*, **48**(16): 420–432.
14. Mao, J.S., Cui, Y.L., Wang, X.H., Sun, Y., Yin, Y.J. and Zhao, H.M. (2004). A Preliminary Study on Chitosan and Gelatin Polyelectrolyte Complex Cytocompatibility by Cell Cycle and Apoptosis Analysis, *Biomaterials*, **25**(18): 3973–3981.
15. Huang, Y., Onyeri, S., Siewe, M., Moshfeghian, A. and Madihally, S.V. (2005). *In vitro* Characterization of Chitosan-Gelatin Scaffolds for Tissue Engineering, *Biomaterials*, **26**(36): 7616–7626.
16. Chen, C.S., Mrksich, M., Huang, S., Whitesides, G.M. and Ingber, D.E. (1997). Geometric Control of Cell Life and Death, *Science*, **276**(5317): 1425–1428.
17. Zhang, S., Yan, L., Altman, M., Lassle, M., Nugent, H., Frankel, F., Lauffenburger, D.A., Whitesides, G.M. and Rich, A. (1999). Biological Surface Engineering: A Simple System for Cell Pattern Formation, *Biomaterials*, **20**(13): 1213–1220.
18. Kane, R.S., Takayama, S., Ostuni, E., Ingber, D.E. and Whitesides, G.M. (1999). Patterning Proteins and Cells Using Soft Lithography, *Biomaterials*, **20**(23–24): 2363–2376.
19. Wang, L., Sun, J., Li, L., Mears, D., Horvat, M. and Sheil, A.R. (1998). Comparison of Porcine Hepatocytes with Human Hepatoma (C3A) Cells for Use in a Bioartifical liver support system, *Cell Transplant.*, **7**(5): 459–468.
20. Dalby, M.J., Childs, S., Riehle, M.O., Johnstone, H.J.H., Affrossman, S. and Curtis, A.S.G. (2003). Fibroblast Reaction to Island Topography: Changes in Cytoskeleton and Morphology with Time, *Biomaterials*, **24**(16): 927–935.

21. Rajaraman, R., Rounds, D.E., Yen, S.P.S. and Rembaum, A. (1974). A Scanning Electron Microscopy Study of Cell Adhesion and Spreading *in vitro*, *Experimental Cell Research*, **88**(2): 327–339.
22. Hughes, R.D. and Williams, R. (1996). Assessment of Bio-Artificial Liver Support in Acute Liver Failure, *Int. J. Artif. Organs*, **19**(1): 3–6.
23. Chen, J.P., Yu, S.C., Hsu, B.R.S., Fu, S.H. and Lin, H.S. (2003). Loofa Sponge as a Scaffold for the Culture of Human Hepatocyte Cell Line, *Biotechnol. Prog.*, **19**(2): 522–527.
24. Kang, I.K., Kim, G.J., Kwon, O.H. and Ito, Y. (2004). Co-culture of Hepatocytes and Fibroblasts by Micropatterned Immobilization of β-galactose Derivatives, *Biomaterials*, **25**(18): 4225–4232.
25. Fukuda, J., Khademhosseini, A., Yeh, J., Eng, G., Cheng, J., Farokhzad, O.C. and Langer, R. (2006). Micropatterned Cell Co-Cultures Using Layer-by-layer Deposition of Extracellular Matrix Components, *Biomaterials*, **27**(8): 1479–1486.
26. Mosmann, T. (1983). Rapid Colorimetric Assay for Cellular Growth and Survival: Application to Proliferation and Cytotoxicity Assays, *J. Immuno. Methods*, **65**(1–2): 55–63.
27. Lobner, D. (2000). Comparison of the LDH and MTT Assays for Quantifying Cell Death: Validity for Neuronal Apoptosis?, *J. Neurosci. Meth.*, **96**(2): 147–152.
28. Ren, J.G., Zheng, R.L., Shi, Y.M., Gong, B. and Li, J.F. (1998). Apoptosis, Redifferentiation and Arresting Proliferation Simultaneously Triggered by Oxidative Stress in Human Hepatoma Cells, *Cell Biology Int.*, **22**(1): 41–49.